Experimental and *ab initio* studies of the reactive processes in gas phase *i*-C$_3$H$_7$Br and *i*-C$_3$H$_7$OH collisions with potassium ions

E. López,[1] J. M. Lucas,[1] J. de Andrés,[1] M. Albertí,[1] J. M. Bofill,[2] D. Bassi,[3] and A. Aguilar[1,a)]

[1]*Departament de Química Física, Institut de Química Teòrica i Computacional (IQTCUB), Universitat de Barcelona, Martí i Franquès, 1, 08028 Barcelona, Spain*
[2]*Departament de Química Orgànica, Institut de Química Teòrica i Computacional (IQTCUB), Universitat de Barcelona, Martí i Franquès, 1, 08028 Barcelona, Spain*
[3]*Dipartimento di Fisica, Università degli Studi di Trento, 38123 Povo-Trento, Italy*

Collisions between potassium ions and neutral *i*-C$_3$H$_7$Br and *i*-C$_3$H$_7$OH, all in their electronic ground state, have been studied in the 0.10–10.00 eV center of mass (CM) collision energy range, using the radiofrequency-guided ion beam technique. In K$^+$ + *i*-C$_3$H$_7$Br collisions KHBr$^+$ formation was observed and quantified, while the analogous KH$_2$O$^+$ formation in K$^+$ + *i*-C$_3$H$_7$OH was hardly detected. Moreover, formation of the ion-molecule adducts and their decomposition leading to C$_3$H$_7^+$ and either KBr or KOH, respectively, have been observed. For all these processes, absolute cross-sections were measured as a function of the CM collision energy. *Ab initio* structure calculations at the MP2 level have given information about the potential energy surfaces (PESs) involved. In these, different stationary points have been characterized using the reaction coordinate method, their connectivity being ensured by using the intrinsic-reaction-coordinate method. From the measured excitation function for KHBr$^+$ formation the corresponding thermal rate constant at 303 K has been calculated. The topology of the calculated PESs allows an interpretation of the main features of the reaction dynamics of both systems, and in particular evidence the important role played by the potential energy wells in controlling the reactivity for the different reaction channels. © *2014 AIP Publishing LLC.* [http://dx.doi.org/10.1063/1.4898377]

I. INTRODUCTION

Ion-molecule reactions are of high interest in different fields of physical chemistry, chemical physics and related areas such as plasma modelling,[1] atmospheric chemistry,[2] biological systems,[3] planetary atmospheres, and interstellar media.[4] In the last years our research group has been dedicated to study both alkali ion-neutral molecule reactive collisions at collision energies in the few keV domain[5] and the same at low energies in the range of the few eV.[6] In the former case, possible reactions are electron transfer ones giving electronically excited alkali atoms, intrinsically non-adiabatic processes where several potential energy surfaces (PESs) are involved,[5,7,8] while at low energies the reactive processes evolve adiabatically on a single PES.[6] Some antecedents of these alkali ion reactions with halogenated hydrocarbons (HHC) and alcohols were the studies done by Allison and Ridge observing their collision induced dehydrohalogenation or dehydration, respectively,[9,10] and the earlier ones by Wieting *et al.* with different organic molecules.[11] Following these studies Creasy and Farrar, among others, considered the dehydration produced when a Li$^+$ beam crosses a sample bulb of *ter*-butanol[12] as well as the *iso*- and *n*-propyl chloride and *iso*-propyl bromide dehydrohalogenations[13] induced by collisions with low energy lithium ions crossing a

supersonic beam of the neutral molecule at a few defined collision energies.

Using a radiofrequency guided-ion-beam (RF-GIB) apparatus built in our laboratory a few years ago[14] we have studied[6,15–17] some of the HHC dehydrohalogenations induced by alkali-ions discussed by Alison and Ridge.[10] In our experiments we measured the excitation functions for different reaction channels observed in reference 10, giving also the measured reactivities for some systems reported there as non-reactive as well as for other reaction channels not explicitly considered in the Allison and Ridge work. Although experimental data can be qualitatively interpreted in terms of the empirical reaction mechanism stated in Ref. 10, later improved in Ref. 13 where a transition state associated with the migration of a hydrogen atom was proposed, a full understanding of the behavior shown by the measured excitation functions was only achieved after doing electronic structure calculations for the PESs where the corresponding reactive processes take place.[6,15–17]

In the present paper we report on the electronic singlet ground state of *i*-C$_3$H$_7$Br and *i*-C$_3$H$_7$OH molecules colliding with ground state K$^+$ inducing their dehydrohalogenation and dehydration reaction, respectively. As in the case of our previous studies, the possible reaction channels that can be expected to take place are

$$K^+ + i\text{-}C_3H_7R \rightarrow [KC_3H_6]^+ + HR, \tag{1}$$

---

a)Author to whom correspondence should be addressed. Electronic mail: a.aguilar@ub.edu. Fax: +34 93 402 12 31.

$$K^+ + i\text{-}C_3H_7R \rightarrow C_3H_6 + KHR^+, \qquad (2)$$

$$K^+ + i\text{-}C_3H_7R \rightarrow C_3H_7^+ + KR, \qquad (3)$$
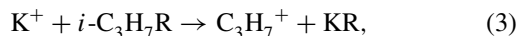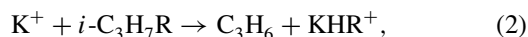
where R represents either Br or OH and HR the HBr produced in the dehydrohalogenation reaction or the H_2O generated in the dehydration one. Equations (1) and (2) represent for each R the two reaction channels leading to the formation of HR and the unsaturated C_3H_6 molecule, which differ in the potassium ion attaching itself to the hydrocarbon in (1) and to the HR in (2).

In addition to reaction channels (1) and (2) which Alison and Ridge did not consider[10] for different HHC and alcohols reactions with potassium ion, reaction channel (3) describes the possible decomposition of the ion-molecule adduct formed in the collision. Such a reaction, involving the heterolytic breakage of the original C–R bond can be expected to be endoergic, so this channel will be open only when the collision energy is large enough and the system's total energy is properly distributed among the vibrational modes of the $[K\text{-}i\text{-}C_3H_7R]^+$ collision complex, thus allowing the C–R bond dissociation. Moreover, when the internal energy content of the $C_3H_7^+$ produced in reaction (3) is great enough it could further decompose[5, 18] through several endothermic reactions, but these have not been observed in the present study.

By performing collision experiments at low enough pressure ensuring single collision conditions, the reaction cross-section energy dependences have been measured for those reactive processes of $i\text{-}C_3H_7Br$ and $i\text{-}C_3H_7OH$ molecules with potassium ions that have been experimentally characterized, as well as the excitation functions for the formation of the $[K\text{-}i\text{-}C_3H_7R]^+$ adducts in the range of low collision energies (hereafter labeled as reaction (4)). Moreover, a detailed electronic structure calculation at the *ab initio* level have been done for both $K^+ + i\text{-}C_3H_7Br$ and $K^+ + i\text{-}C_3H_7OH$ collision systems obtaining detailed information of the PES on which the respective reaction processes evolve. After the introduction the paper is structured as follows: Sec. II reports on the experimental part with a short description of the experimental setup followed by experimental measured reactive cross-section energy dependences. The relevant information on PES topology obtained by *ab initio* structure calculations can be seen in Sec. III. Finally, in Sec. IV we present the discussion and interpretation of the experimental results in the light of the structure calculations, while conclusions are given in Sec. V.

II. EXPERIMENTAL

A. Brief description of the experimental setup and center-of-mass cross-sections

The experimental equipment used in the present work is a RF-GIB apparatus that has been described previously[14] so only a brief outline is given here. As recently commented,[5] a quadrupole mass filter has been inserted between the ion source and the reaction cell that allows selecting specific mass/charge ions by removing undesired contaminant ions. In the present case a pure $^{39}K^+$ ($^1S_0$) beam is generated by

thermionic effect on a suitable device (HeatWave Laboratories) heated at some 1200 K. The extracted ions, mass filtered by the first quadrupole, are collimated and focused into an octopole ion guide shielded by a stainless steel sleeve which doubles as the gas cell, the thermal target gas being introduced there at low pressure. The octopole field both guides the primary ions and gathers the products in a 4π solid angle. Both parent and product ions are refocused on exiting the octopole, selected by a second quadrupole mass analyzer and detected by a secondary electron multiplier (SEM). Pure and dry $i\text{-}C_3H_7R$ vapors are introduced in the scattering cell through a vacuum pipeline controlled by a fine-pitch needle valve. Along the experiment the gas cell pressure is kept at around few 10^{-5} mbar, low enough to ensure single-collision conditions and keeping the background pressure in the range of 10^{-6}–10^{-7} mbar. All systems and ancillary electronics are PC-controlled with a software developed in our group using LabVIEW (©) National Instruments).

In the laboratory frame (LF) of the RF-GIB apparatus the kinetic energy of the potassium ions (E_{lab}) is given by the difference between the DC extraction potential and the DC voltage supplied to the octopole bars. The zero of these energies as well as their uncertainty are determined using the so-called retarding potential analysis method[19] where the octopole ion guide acts as the retarding energy analyzer and the following equation is used to correct the LF kinetic energy, especially at low values:

$$\bar{E}_{lab} = \int_0^\infty E \cdot P(E, E_{lab}) dE, \qquad (4)$$

where $P(E, E_{lab})$ is the normalized distribution of the ion beam energy (E) depending on the nominal energy (E_{lab}) measured in the LF. The energy distribution for this kind of processes is nearly Gaussian[19, 14] and in the present experiments, the full-width at half-maximum (FWHM) for K^+ is around 0.30 eV. Assuming that target molecules are stationary, for a given ion LF energy, the corresponding center of mass (CM) relative kinetic energy E_0 is given by the well-known expression,

$$E_0 = \bar{E}_{lab} \frac{m_B}{m_B + m_I}, \qquad (5)$$

where m_I and m_B are the masses of the ion and of the neutral molecule, respectively. In fact, target molecules are not stationary but have a random thermal motion. This leads to an energy distribution that for a given ion energy (E_o) suffers an associated Doppler broadening[20–22] proportional to the square root of the energy, so its relative importance lessens when energy increases. However, it does lead to a difference between true $\sigma(E_0)$ and measured $\sigma_{eff}(E_0)$ reaction cross-sections,[19] to which we will refer in our cross-sections measurements.[17] For a given CM collision energy E_0 the measured cross-section $\sigma_{eff}(E_0)$ is given by

$$\sigma_{eff}(E_0) = \frac{I_i}{I_0 n l}, \qquad (6)$$

where n is the target gas density in the collision cell and l the effective path length. Both n and l values had been obtained in a previous calibration experiment[23] by comparing our

results with those described by Koizumi and Armentrout.[24] Using this procedure cross sections can be measured in absolute units, but with an uncertainty of around 30% or even larger.

B. $K^+ + i\text{-}C_3H_7Br$ and $K^+ + i\text{-}C_3H_7OH$ reactive cross section measurements

Prior to the cross section determinations, a mass analysis scan at different energies has been done in the 1–200 mass/charge (m/z) units range. For the system $K^+ + i\text{-}C_3H_7Br$, signals have been detected at 161, 81, 119, and 43 m/z that can be associated with $[K\text{-}i\text{-}C_3H_7Br]^+$, $[KC_3H_6]^+$, $[KHBr]^+$, and $C_3H_7^+$ ions (corresponding to the ^{79}Br atomic isotope), as well as the 39 m/z signal for primary potassium ion beam. The isotopic counterparts for the ^{81}Br have been observed with a signal ratio nearly identical to the natural isotopic abundance of bromine atoms. In the case of the $K^+ + i\text{-}C_3H_7OH$ collision system, signals at 99, 57, 43, and 39 m/z units were detected and associated with $[K\text{-}i\text{-}C_3H_7OH]^+$, $[KH_2O]^+$, and $C_3H_7^+$ products and the primary potassium ion signal, respectively. As an overall trend, results for the systems considered here show much lower product intensities than those corresponding to the $K^+ + i\text{-}C_3H_7Cl$ system previously studied[6] (about two orders of magnitude depending on the ion product considered) using the same experimental setup. Moreover, possible ion products $C_2H_3^+$ and $C_3H_5^+$ (present in $K^+ + i\text{-}C_3H_7Cl$ collisions) resulting from the decomposition of highly vibrationally excited $C_3H_7^+$ produced in reaction (3) were not observed in the present study. Therefore, very low reactivity can be expected for dehydrohalogenation and dehydration reactions considered here. For example, the $[KC_3H_6]^+$ signal was not observed at all in $i\text{-}C_3H_7OH$ or $i\text{-}C_3H_7Br$ reactions; although detected in the mass scan, its intensity was so low as to make impossible to gather an excitation function for this channel.

The excitation function for reaction (2) leading to the formation of $[KHBr]^+$ in $K^+ + i\text{-}C_3H_7Br$ collisions in the CM 0.10–6.00 eV energy range is shown in Fig. 1(b) together with that for $[K\text{-}i\text{-}C_3H_7Br]^+$ adduct formation (Fig 1(a)). On the other hand, the excitation function for $C_3H_7^+$ formation by adiabatic (see Sec. III) decomposition of the $[K\text{-}i\text{-}C_3H_7Br]^+$ adduct (reaction (3)) is shown in Fig 1(c). As it can be appreciated from Fig. 1 the excitation functions for $[K\text{-}i\text{-}C_3H_7Br]^+$ and $[KHBr]^+$ formation are of the same order of magnitude and roughly two orders smaller than those measured[6] for adduct formation in $K^+ + i\text{-}C_3H_7Cl$ collisions. Moreover, in this previous study, the analogous reaction (2) producing $[KHCl]^+$ was not observed. Cross-section values for $[KHBr]^+$ are roughly of the same order of magnitude than those for the decomposition $C_3H_7^+ \rightarrow C_3H_5^+ + H_2$ observed in $K^+ + i\text{-}C_3H_7Cl$ collisions but not detected in the bromide's case. As shown in Fig. 1(b) the excitation function for $[KHBr]^+$ formation has an experimental energy threshold of around 1.10 eV, describes a maximum around 2.50 eV, and becomes negligible over 5.00 eV. The excitation function for reaction (3) as shown in Fig. 1(c) has an energy dependence similar to that measured
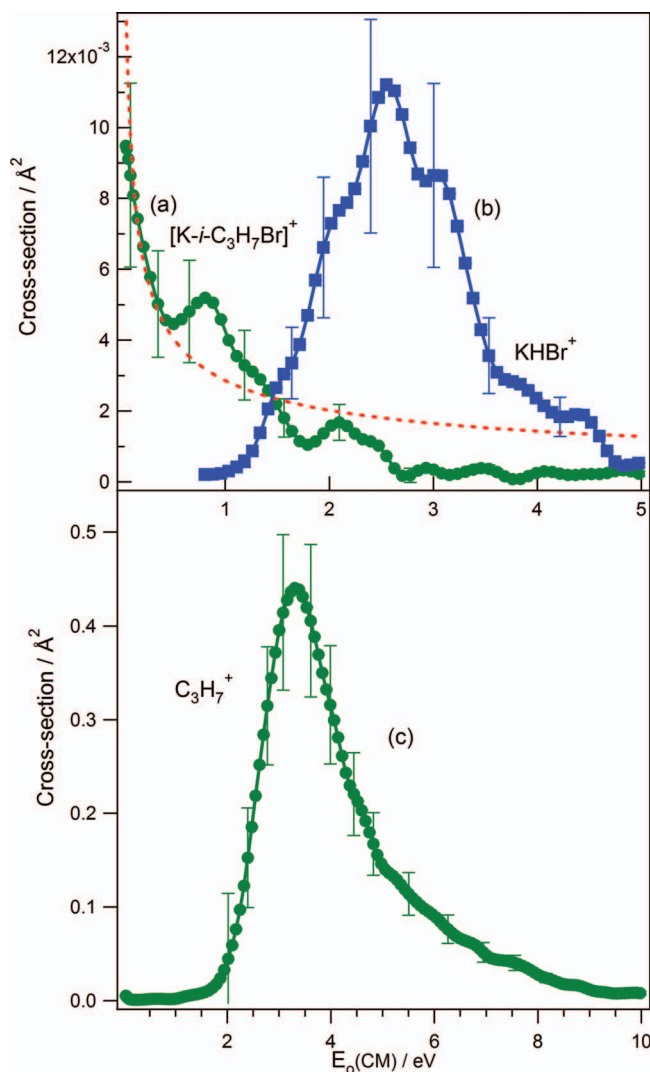

FIG. 1. Cross-section CM energy dependences in $K^+ + i\text{-}C_3H_7Br$ collisions for: (a) $[K\text{-}i\text{-}C_3H_7Br]^+$ adduct formation (green circle); (b) dehydrohalogenation reaction (2) (blue square); and (c) reaction (3). Discontinuous line: LGS model scaled to experimental values at low energies (see text). All energies are given in the CM frame.

in the $i\text{-}C_3H_7Cl$ studies.[6, 17] Its experimental energy threshold can be estimated at some 1.80 eV, and the shape displays a maximum around 3.00 eV followed by a relatively smooth and wide decay, becoming negligible at energies higher than 10.00 eV. Measured cross-section values for the formation of $C_3H_7^+$ by $[K\text{-}i\text{-}C_3H_7Br]^+$ decomposition are roughly one order of magnitude lower that the corresponding ones[6] for $[K\text{-}i\text{-}C_3H_7Cl]^+$.

Experimental results obtained in $K^+ + i\text{-}C_3H_7OH$ reactive collisions are shown in Fig. 2 in the CM 0.10–8.00 eV energy range. In Fig. 2(a) the cross-section vs. energy dependence for $[K\text{-}i\text{-}C_3H_7OH]^+$ formation is given, while Fig. 2(b) shows the excitation function for reaction channel (3). It can be appreciated from these figures that reaction cross-section values for the adduct formation are of the same order of magnitude that in $K^+ + i\text{-}C_3H_7Cl$ previously considered collisions and roughly two orders higher than in the $K^+ + i\text{-}C_3H_7Br$ system. As regards to the dehydration
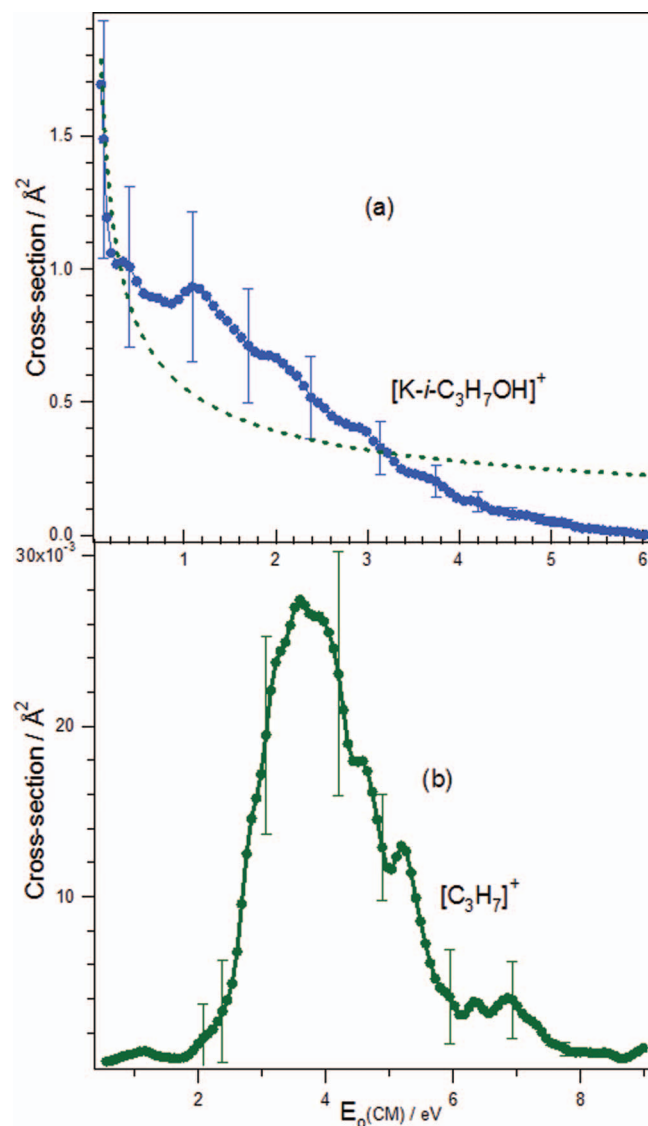
FIG. 2. Cross-section CM energy dependences in $K^+ + i\text{-}C_3H_7OH$ collisions for: (a) $[K\text{-}i\text{-}C_3H_7OH]^+$ adduct formation and (b) reaction (3). Discontinuous line: LGS model scaled to experimental values at low energies (see text). All energies are given in the CM frame.

channel (2) leading to $[KH_2O]^+$ observed in the mass scan analysis, its low measured intensity and signal-to-noise ratio precluded gathering a reliable excitation function for reaction (2) in $K^+\text{-}i\text{-}C_3H_7OH$ collisions. The cross-section numerical values for $[K\text{-}i\text{-}C_3H_7OH]^+$ decomposition reaction (Fig. 2(b)) are roughly one order of magnitude lower than in the $K^+ + i\text{-}C_3H_7Br$ case. Considering excitation functions for the ion-molecule adduct formation, although differing in order of magnitude, both systems show decreasing cross-section values when the collision energy increases and no energy threshold, as expected in ion-molecule reactions, controlled by non-covalent long-range interaction potentials. From this adduct, located in the entrance valley of the PES containing the potential well which stabilizes the ion-molecule collision complex, different reactive channels can be expected such as those indicated by reactions (1)–(3) in our case, each one satisfying its own energy requirement.

III. ELECTRONIC STRUCTURE CALCULATIONS

A full understanding of the experimental data requires the knowledge of the behavior and the topology of the PES on which the reactive processes take place. In the present case, considering the closed shell electronic configuration of K^+, $i\text{-}C_3H_7Br$, and $i\text{-}C_3H_7OH$, and assuming that the reactions we are dealing with do proceed adiabatically, we have studied the ground singlet PES associated with the reactive supermolecule corresponding to each one of the ion-molecule systems considered. The main topology features of these PESs have been obtained by performing *ab initio* calculations at the second order Möller-Plesset (MP2)[25] level of theory using the electronic structure GAUSSIAN package[26] and the Pople's 6-31G basis set including p polarization functions for each hydrogen atom and on each heavy atom as implemented in the computer code. The minimum energy path (MEP)[28] on the potential surface has been obtained using the reaction co-ordinate method[27] and different stationary points have been characterized along the reaction pathway. Applying the intrinsic reaction coordinate (IRC)[29] method the connectivity of the different stationary points along the MEP has been confirmed in each case.

A. *Ab initio* characterization of the ground singlet PESs for $[K–i\text{-}C_3H_7Br]^+$ and $[K–i\text{-}C_3H_7OH]^+$ reactive systems

Ab initio calculations for all reactant and product molecules involved in reactions (1)–(3) for R = Br, OH have been done separately for their ground singlet state doing a full optimization of their geometries. The Hessian matrix analysis of these optimized structures confirmed that they are true stationary points describing a potential energy well, and their zero point harmonic energies, as provided by the Gaussian code, have been calculated. Thus, the reaction energies ($\Delta_r E$) and the associated reaction enthalpies at zero Kelvin ($\Delta_r H_0$) have been obtained as shown in Table I for reactions (1)–(3) in $K^+ + i\text{-}C_3H_7Br$ and $K^+ + i\text{-}C_3H_7OH$ reactive collisions.

As can be appreciated in Table I, for the $K^+ + i\text{-}C_3H_7Br$ collision system, reactions (1) and (2) are both endothermic with similar $\Delta_r H_0$ values, while reaction (3), also endothermic, has a relative high reaction enthalpy, about five times larger than those for (1) and (2). For the reaction energies ($\Delta_r E$) a similar trend was also found, although the inclusion of the zero point energy (ZPE) clearly reduces the energetic requirement for all reactions. For the $K^+ + i\text{-}C_3H_7OH$ reactive system it can be seen from the same table that reaction (1) is endothermic, reaction (2) is exothermic while reaction

TABLE I. Calculated reaction energies ($\Delta_r E$) and 0 K reaction enthalpies ($\Delta_r H_0$) for each reaction channel in $K^+ + i\text{-}C_3H_7Br$ and $K^+ + i\text{-}C_3H_7OH$ reactive collisions. All values are given in eV.

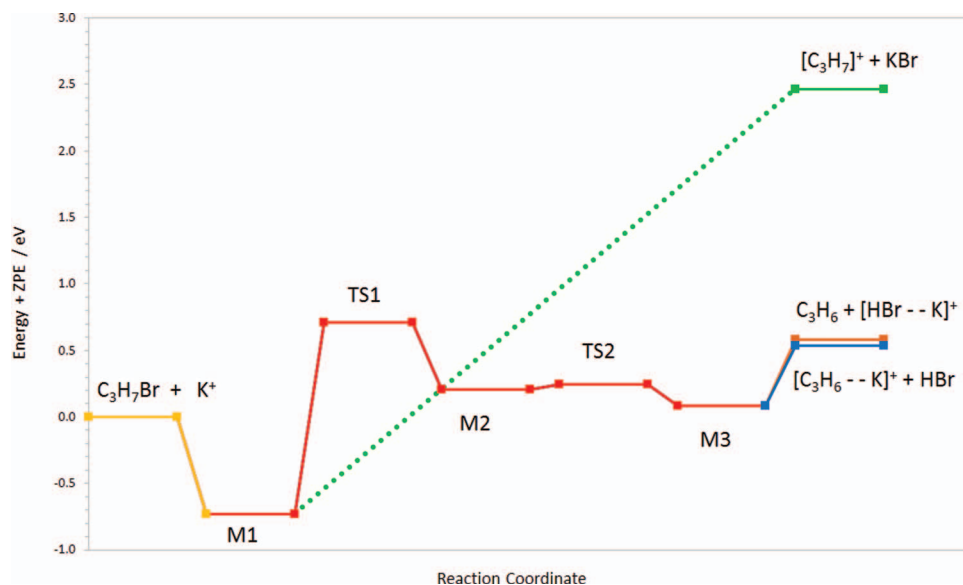|	$K^+ + i\text{-}C_3H_7Br$ $\Delta_r E (\Delta_r H_0)$	$K^+ + i\text{-}C_3H_7OH$ $\Delta_r E (\Delta_r H_0)$
Reaction (1)	0.764 (0.535)	0.438 (0.246)
Reaction (2)	0.803 (0.579)	−0.011 (−0.161)
Reaction (3)	2.624 (2.465)	4.702 (4.442)

FIG. 3. Schematic ZPE profile along the minimum energy path characterized at the MP2 level on the ground singlet PES of the (K-*i*-C$_3$H$_7$Br)$^+$ reactive system, showing the different minima (M) and transition states (TS) and their IRC connectivity (reactants ZPE taken at origin): Continuous (light yellow) line describes the asymptotic region from reactants to the M1 adduct formation; continuous (red) line describes the intermediate interaction region of the PES from M1 to M3; continuous (blue) and (dark yellow) lines connect M3 with the asymptotic reactions (1) and (2), respectively; dotted line (green) indicates the reaction pathway from M1 to reaction decomposition products (3).

(3) is very endothermic, practically twice the corresponding value for *i*-C$_3$H$_7$Br.

After calculating the reaction energies, the strategy to characterize the PES proceeds by localization of the stationary points. This has been done by a detailed Hessian matrix analysis, confirming their nature as either transition states (TS) or minima (M). A schematic representation along the MEP of the stationary points relevant to each reaction considered is given in Figs. 3 and 4, where energy values are referred to the reactants one including always the ZPE of each stationary point (see Table II). In these figures it can be seen that both reactive systems show qualitatively common features along their MEPs energy profiles. Starting from the reactants asymptotic region, the reacting supermolecule
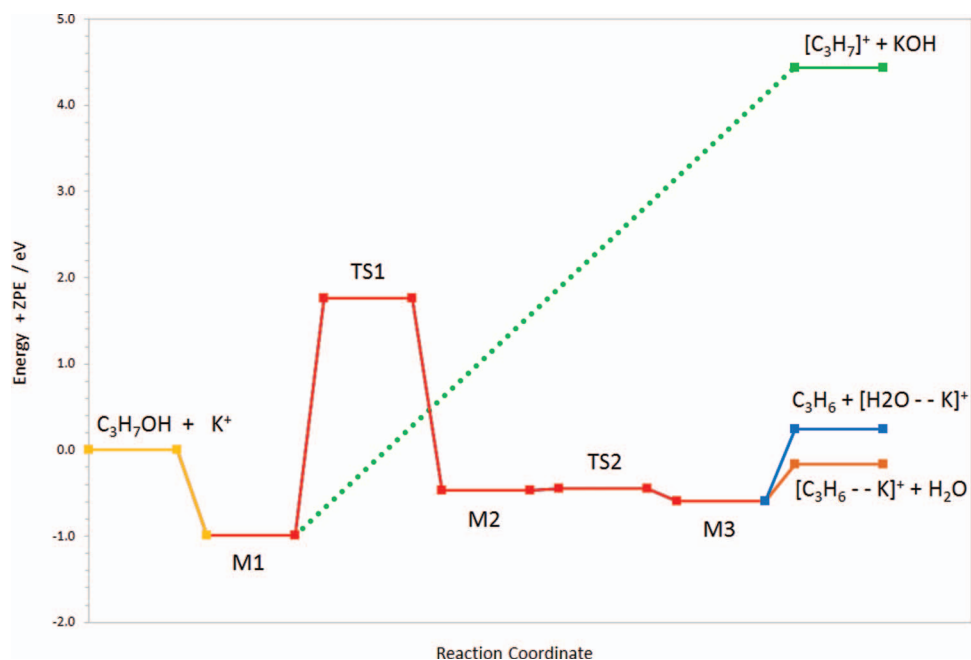

FIG. 4. Schematic ZPE profile along the minimum energy path characterized at the MP2 level on the ground singlet PES of the (K-*i*-C$_3$H$_7$OH)$^+$ reactive system, showing the different minima (M) and transition states (TS) and their IRC connectivity (ZPE of reactants taken a the origin): Continuous (light yellow) line describes the asymptotic region from reactants to the M1 adduct formation; continuous (red) line describes the intermediate interaction region of the PES from M1 to M3; continuous (blue) and (dark yellow) lines connect M3 with the asymptotic reactions (1) and (2), respectively; dotted line (green) indicates the reaction pathway from M1 to decomposition products (3).

TABLE II. 0 K energies (H_0 = Electronic energies + ZPE) and ZPEs of the stationary points located on the PESs of the $K^+ + i\text{-}C_3H_7Br$ and $K^+ + i\text{-}C_3H_7OH$ reactive systems (referred to the reactants' H_0). All values are given in eV.

		$K^+ + i\text{-}C_3H_7Br$	$K^+ + i\text{-}C_3H_7OH$
Reactants	H_0	0	0
	ZPE	2.647	3.034
M1	H_0	− 0.731	− 0.993
	ZPE	2.655	3.063
TS1	H_0	0.708	1.759
	ZPE	2.491	2.836
M2	H_0	0.205	− 0.464
	ZPE	2.465	2.931
TS2	H_0	0.248	− 0.450
	ZPE	2.459	2.920
M3	H_0	0.0831	− 0.590
	ZPE	2.455	2.903

$[K\text{–}i\text{-}C_3H_7R]^+$ leads to the formation of ion-molecule adducts associated with a potential energy well (M1, see Figures 3 and 4 for R = Br, OH, respectively) without surmounting any potential energy barrier, the K^+-alcohol adduct being more stable (0.262 eV) than the K^+-bromide one.

Analyzing in detail the *ab initio* chemical structure calculations it is found that $[K\text{–}i\text{-}C_3H_7Br]^+$ formation adduct in its equilibrium geometry slightly increases the Br–middle C atom distance (from 1.979 Å to 2.021 Å) while the geometrical structure of the rest of the molecule remains essentially unaltered with a K^+-Br distance of 3.186 Å and a C–Br–K angle of 123.5° (see M1 in Fig. 5). This adduct formation modifies the C_3H_7Br electronic density distribution and the corresponding atomic charges (in terms of the atomic polar tensor (APT)[30,31] atomic charges) as is the case of the Br atom that changes from −0.309 to −0.465 and that of the potassium ion which decreases from 1 to 0.972. Thus, approaching the potassium ion to the bromine, the electronic density on this atom increases and simultaneously a small fraction of the positive charge of the ion is neutralized. At the same time the net charge on the central C atom changes from 0.395 in the free molecule to 0.538 in the adduct, consequently increasing the polar character associated with the middle C–Br bond. This effect can be interpreted in terms of typical long-range induction forces between the initial ion and the neutral polar and polarizable molecule. Moreover, calculated molecular orbitals show a very small overlap of the potassium-centered atomic orbitals and the molecule-centered ones, in agreement with an essentially non-covalent ion-molecule interaction found in other alkali ion-molecule adducts.[32,33] Similar results are found for the $[K\text{–}i\text{-}C_3H_7OH]^+$ adduct (see Figs. 6(a) and 6(b)) with very small geometrical changes compared to the neutral $i\text{-}C_3H_7OH$ molecule: the middle C–OH distance changes from 1.431 Å to 1.458 Å while the O–H one remains essentially the same (from 0.965 Å to 0.967 Å). The K–O distance is 2.593 Å, shorter than the K-Br one in the $[K\text{–}i\text{-}C_3H_7Br]^+$ adduct, as expected since bromine size and polarizability are higher than oxygen ones. In this adduct the potassium ion is located in the opposite direction to the OH, minimizing the Coulomb repulsions between their positive charges (0.965

and 0.278 for potassium and hydrogen, respectively). The coordination of K^+ to the OH group leads to a slight increase in the acid character of its hydrogen atom whose net charge rises from 0.239 in $i\text{-}C_3H_7OH$ to 0.278 in the adduct, the oxygen net charge increasing from −0.609 to −0.724, thus increasing also the polar character of the C–OH bond in the adduct. The inspection of the atomic contribution to the molecular orbitals of the adduct shows that, as in the case of $[K\text{–}i\text{-}C_3H_7Br]^+$, adduct orbitals of the potassium fragment do not overlap significantly with those of the $i\text{-}C_3H_7OH$, showing that in both adducts ion-molecule interactions are mainly non-covalent.

From the ZPE profiles of the PES along the reactants-to-products MEP in $K^+ + i\text{-}C_3H_7Br$ and $K^+ + i\text{-}C_3H_7OH$, shown, respectively, in Figures 3 and 4, after M1 adduct formation it appears a maximum that is a first order saddle point associated with the corresponding transition state TS1. As given in Table II the TS1 zero point potential energy barrier for $K^+ + i\text{-}C_3H_7Br$ is lower than half that for reaction $K^+ + i\text{-}C_3H_7OH$.

Looking closely at the geometrical evolution of the $[K\text{–}i\text{-}C_3H_7Br]^+$ supermolecule from M1 to TS1 (see Figure 5(a)) along the IRC, the K^+ influence on the remaining structure is clear: it promotes the middle C–Br distance increase (from 2.021 Å in M1 to 3.057 Å in TS1) with a simultaneous rotation of one CH_3 group that places one of its H atoms at 2.309 Å from the bromine, simultaneously increasing the corresponding C–H distance (from 1.087 Å in M1 to 1.178 Å in TS1). During this process the potassium ion reduces its distance to the bromine from 3.186 Å to 2.993 Å. From this stationary point the IRC evolution along the reaction path leads to another, very shallow, potential energy well associated with the M2 structure shown in Fig. 5. From this figure it can be appreciated that both C_3H_6 and HBr (Fig. 5(b)) have been essentially formed there by K^+-induced dehydrohalogenation (see Figs. 5(a) and 5(b)). At this point, the supermolecule can easily evolve along a reaction path overcoming a relatively low potential energy barrier (0.043 eV over the M2 minimum) and in this transition state (TS2) the HBr part of the supermolecule approaches its H atom to the central carbon up to 2.322 Å, simultaneously approaching the potassium to the C=C double bond generated by the reaction. From this TS2 structure the evolution of the overall system along the MEP leads to a new potential energy well (M3), more stable than M2, that can be associated to an adduct resulting from the interaction of the potassium ion with the product molecules. The geometry structure of the M3 adduct (see Fig. 5(a)) shows that the potassium ion is on one side coordinated to the center of the C_3H_6 double bond and on the other side to the HBr bromine atom. In this adduct structure the APT net charges are 0.911 on the potassium center, −0.174 on the terminal double bonded carbon atom, and −0.162 on the bromine atom, while for the methyl carbon and for the C-central one, charges are approximately zero. Such a distribution of the atomic charges in M3, in addition to the fact that atomic orbitals of the potassium center practically no dot participate in the occupied molecular orbitals of the supermolecule, explain the stability of this structure, essentially in terms of electrostatic long-range interactions and of its non-covalent nature as in the case of the reactants adduct M1 between the K^+ and $i\text{-}C_3H_7Br$.
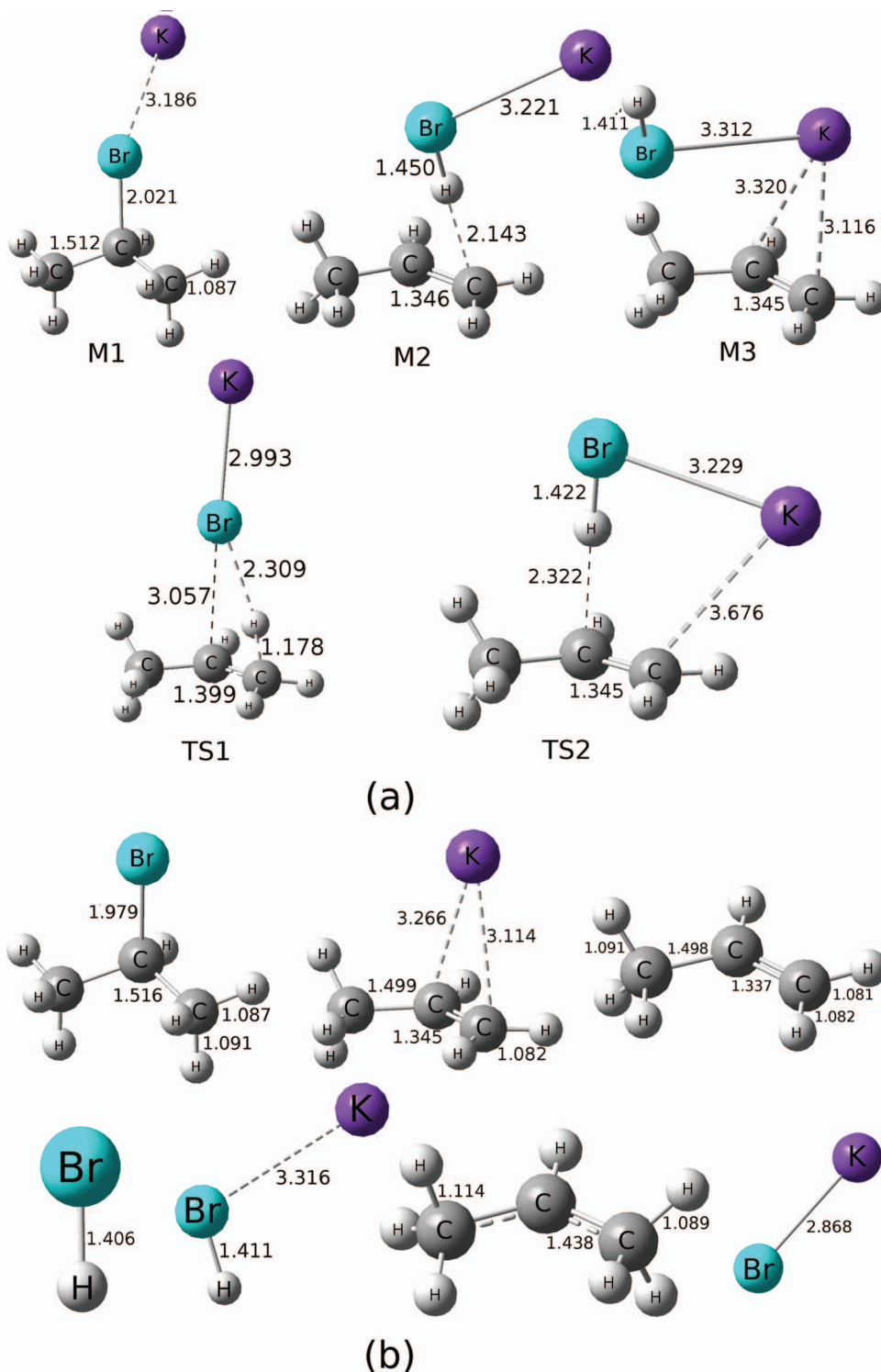
FIG. 5. Optimized geometry structures at the MP2 level characterized on the ground singlet PES of the (K-*i*-C$_3$H$_7$Br)$^+$ reaction system: (a) for the different stationary points, minima (M) and transition states (TS) and located along the IRC reaction pathway shown in Fig. 3; (b) for reactants and products in the different reaction channels. For simplicity only the most relevant interatomic distances (in Å) are shown (see text).

From the structure of the M3 adduct the products for reactions (1) and (2) are formed by simply increasing either the Br–K distance or the K–C$_3$H$_6$ one, respectively. As shown in Fig. 3 and Table II, the asymptotic collision exit channels associated with reactions (1) and (2) are both endothermic, with (2) being 0.039 eV more endothermic than (1). However, the same figure shows that both asymptotic reactions are

below the TS1 potential energy barrier, so it can be expected that the energy requirements for both reactions will be controlled by the height of the barrier associated with the first saddle point along the reaction path instead of by their own endothermicity.

Fig. 6 shows the geometrical structures associated with the different stationary points located on the PES of the K$^+$
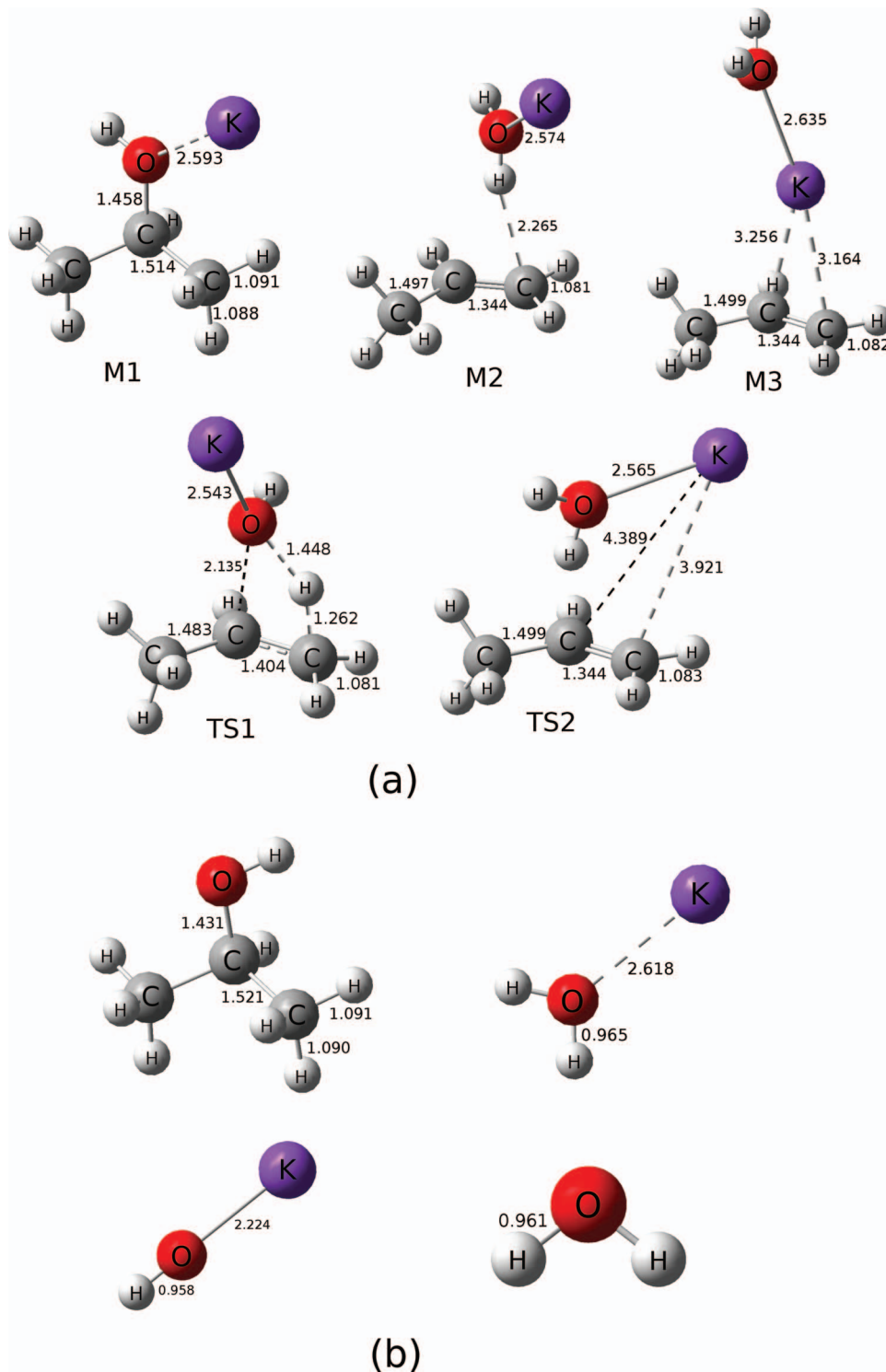
FIG. 6. Optimized geometry structures at the MP2 level characterized on the ground singlet PES of the (K-*i*-C$_3$H$_7$OH)$^+$ reaction system: (a) for the different stationary points, minima (M) and transition states (TS) and located along the IRC reaction pathway shown in Fig. 3; (b) for reactants and products in the different reaction channels. For simplicity only the most relevant interatomic distances (in Å) are shown (see the text) and those for [KC$_3$H$_6$]$^+$, C$_3$H$_6$, and C$_3$H$_7$$^+$ given in Fig. 5 omitted.

+ *i*-C$_3$H$_7$OH reaction (Fig. 4) corresponding to all potential energy wells or transition states along the MEP. As can be seen in Fig. 6(a) the potassium ion is practically positioned in the H-O-C plane and over the carbon atom of the CH$_3$ group. In this arrangement the K$^+$ positive net charge interacts attractively with the negative one of the oxygen, while electro-static interaction with the CH$_3$ group is negligible since both carbon and hydrogen have approximately zero net charge. In M1 the structure of the C$_3$H$_7$OH fragment is only slightly distorted with respect to that of the reactant molecule. From M1 and evolving along the IRC to the saddle point TS1, the CH$_3$ group which will provide the H atom involved in the

dehydration process (here designated as H*) rotates around the C–C bond and simultaneously both middle C–O and C–H* distances increase up to 2.135 Å and 1.262 Å, respectively, while the O–H distance remains nearly unchanged. In this TS1 geometry the O–H* distance is 1.448 Å, the potassium approaches to the oxygen atom by around 0.05 Å respect to its value in M1 and the middle C–CH_3 bond decreases from 1.514 in M1 to 1.404 Å in TS1. In Fig. 6(a) it can also be appreciated that, although with a much lengthened O-H distance, an incipient H_2O is going to be formed.

From TS1 the evolution along the reaction coordinate of the reactive supermolecule leads to a new potential energy well (M2) on the PES whose geometric structure is shown in Fig. 6(a) where it is clear the formation of a H_2O molecule trapped between the potassium center and the coproduced CH_3–CH=CH_2 molecule. From the figure it can be seen that the new formed O–H water bond is oriented to the formed double bond, the H* to terminal double bond C atom distance being 2.265 Å. The positive charge on the H* (0.409), attractively interacting with the net charge on the terminal double bond carbon (−0.156); the small charge on the middle C (0.034) and the oxygen charge (−0.728) which interacts attractively with that of the potassium (0.974) justify the relative stability of this structure. The evolution of the reactive supermolecule from the M2 minimum along the reaction coordinate can be associated with a reorientation of the H_2O-K plane with the O-K distance remaining constant (2.565 Å in TS2) while the potassium tends to approach the terminal double bond carbon (with net charges 0.967 and −0.161, respectively). This leads to the transition state TS2 whose geometry is also given in Fig. 6(a). From this structure the supermolecule easily evolves along the IRC pathway leading to the more stable (M3) geometric arrangement where the potassium center (net charge 0.922) lies between the H_2O molecule (with the oxygen atom oriented to the potassium) and the unsaturated molecule. In this adduct the distances of the potassium center to the terminal double bond carbon atom and to the central carbon atom differ only in 0.092 Å, with the potassium being located nearly over the center of the electronic cloud associated with the π-bond between carbon atoms of the CH_3–CH=CH_2 fragment of M3. From this structure, where the potassium center is coordinated to both H_2O and CH_3–CH=CH_2 molecules, by simply increasing the potassium double bond carbon atoms distance or the potassium-oxygen distance, products in reaction channels (1) and (2), respectively, are generated without the appearance of any potential energy over the endothermicity of the process.

In addition to reactions (1) and (2), reaction (3) has been also characterized for both the dehydrohalogenation and the dehydration reactions. Starting with the M1 equilibrium geometry of the ion-molecule adduct, where the potassium is coordinated to the bromine atom of the *i*-C_3H_7Br or to the oxygen atom of the *i*-C_3H_7OH, and continuously increasing the middle C–Br or the middle C–O distances, respectively, the supermolecule adiabatically decomposes giving $C_3H_7^+$ + KBr for the former system or $C_3H_7^+$ + KOH for the latter. Along the whole reaction path, which always conserves its singlet multiplicity character, and increasing the middle C–R distance, the C_3H_7 fragment increases its global net charge

until the formation of $C_3H_7^+$ and the neutral KBr or KOH products. Along the MEP no potential energy barriers appear, so that the systems need only to overcome the reaction endothermicity. From Table I it can be seen that the calculated $\Delta_r H_0$ value for reaction (3) in the case of K^+ + *i*-C_3H_7Br is in a good enough agreement with the experimentally estimated value (2.25 eV[34]) while for K^+ + *i*-C_3H_7OH system the experimental estimated value (3.54 eV[34]) does differ more with the calculated one.

IV. DISCUSSION ON THE POTASSIUM ION REACTIONS WITH *i*-C_3H_7Br AND *i*-C_3H_7OH

The interaction between an ion and a neutral molecule (such as those reported here) is expected to proceed via an ion-molecule collision complex that, in terms of chemical kinetics mechanisms, can be associated with the formation of reaction intermediates evolving finally to the different reaction products. Several intermediates, characterized as potential energy wells, are found along the evolution of the collision complex from reactants to products on the reaction PES. These are explored and lead successively to different reaction products, assuming that the collision complex has enough energy to satisfy the energetic requirements, such as those imposed by the possible potential energy barriers or by the endothermicity of the reaction. Taking into account that dehydrohalogenations and dehydrations are relatively complex reactions, involving the breakage of two original bonds and the formation of new single and double chemical bonds, the ion-molecule collision complex can be expected to suffer dramatic changes in its chemical structure during its lifetime. The changes of those structures correlating with potential well minima on the reaction PES are evidenced by considering the *ab initio* potential energy profiles (in terms of ZPEs) shown in Figure 3 for K^+ + *i*-C_3H_7Br and in 4 for K^+ + *i*-C_3H_7OH, and the chemical structures given in Figures 5 and 6.

As can be inferred from Figures 3 and 4, independently of the exo- or endothermic character of reactions (1) and (2), the presence of the potential energy barrier associated with TS1 imposes nominal energy thresholds of around of 0.71 eV and 1.76 eV for dehydrohalogenation and dehydration, respectively. For ion-molecule collisions with a total energy content below those nominal energy thresholds, it can be expected that signals strengths measured at *m/z* of 161 and 99 units (attributable to [K–*i*-C_3H_7Br]$^+$ and [K–*i*-C_3H_7OH]$^+$, respectively) decrease as the collision energy increases, since the PESs do not show potential energy barriers between asymptotic reactants and M1. This would mean that the dominant interactions are those associated with electrostatic long-range interactions between partners as is the case for the interaction between the closed shell potassium ion and the polarizable target molecules which also include a permanent electric dipole. Taking into account that the halogenated and alcohol molecules considered here are highly polarizable (9.60 Å^3 and 7.61 Å^3, respectively),[35] it can be assumed in a first approach that, at low collision energies, adduct formation proceeds according to the Langevin-Giousmousis-Stevenson (LGS)[36] capture model whose cross-section energy dependences are shown in Figures 1(a) and 2(a), respectively. As can be seen

in Fig. 1(a) this dependence is in relatively good agreement with the experimental measured values in the lower energy range until around 0.70 eV (CM) but differ at higher collision energies. A similar behavior is also found for the dehydration as can be seen in Fig. 2(a). At low CM energies the collision complex can only explore the region of the PES connecting the reactants entrance valley and the potential energy well M1 and can be considered as a single molecule with a high energy content compared to M1. In the experimental conditions the time of flight of the collision complexes from the reaction cell to the detector is in the range of 10^{-3}–10^{-4} s so that part of them can back-dissociate into reactants during their flight to the detector, remaining then undetected. Although complex lifetime depends on the specific values of its total energy, on total angular momentum and on the couplings between the different degrees of freedom of the supermolecule, an internal energy redistribution, usually lasting picoseconds,[37] can occur. Under these experimental conditions the measured excitation function, at least at low energies, can be associated to the formation of true M1 ion-molecule adducts whose equilibrium geometries are shown in Figures 5(a) and 6(a). On increasing the collision energy, the excitation functions associated to the collision complexes (reactions (4)) tend to decrease, as expected due both to their higher dissociation probability and to the opening of reaction channels (1) and (2).

For collision energies higher than TS1, reactions (1) and (2) can take place and this is the case of the excitation function shown in Fig. 1(b) for KHBr$^+$ formation, which has an experimental energy threshold in agreement with the nominal one that can be expected from the ZPE of its transition state TS1. Moreover, the reactivity of this channel is very small and of the same order of magnitude than those for adduct formation at these energies. In the same figure it can be seen how, in the same collision energy range where KHBr$^+$ formation starts to increase, the cross-section values for [K–i-C$_3$H$_7$Br]$^+$ do also increase slightly. A plausible explanation for this fact would be that, at collision energies slightly higher than the TS1 one, the reacting supermolecule, in progressing to products, can also explore that part of the PES which contains potential energy wells M2 and M3. These, although less attractive than M1, do also contribute to the collision complex stabilization. When the collision energy increases still more this signal tends again to decrease, as can be expected since the collision complex tends to decompose more readily. The excitation function for KHBr$^+$ formation shows the typical energy dependence of a reaction having a threshold energy, with a maximum at around 2.50 eV and then decreasing to negligible values. Taking into account that KHBr$^+$ calculated dissociation energy at 0 K is 0.43 eV, the excitation function behavior can be in part justified by the lower probability of ion-molecule complex formation when the collision energy increases, and also because, at energies high enough, KHBr$^+$ can dissociate into HBr + K$^+$, further decreasing the overall measured reactivity of reaction (2). A similar feature was also found in the excitation function for [K–i-C$_3$H$_7$OH]$^+$ formation, but measured cross-sections are about two orders of magnitude larger. A possible qualitative interpretation of this difference can be given considering that the potential energy well M1 for [K–i-C$_3$H$_7$OH]$^+$ is deeper (about 0.26 eV)

than that for the [K–i-C$_3$H$_7$Br]$^+$ and, consequently, there is a stronger –OH-K$^+$ interaction which stabilizes the adduct and moreover reduces its density of states at a given total energy, consequently hampering its back decomposition into reactants.

As to reaction (2) for K$^+$ + i-C$_3$H$_7$OH, it proved impossible to obtain reliable cross-sections for KH$_2$O$^+$. Such an impossibility can be at least partially justified since the calculated dissociation energy of KH$_2$O$^+$ into K$^+$ and H$_2$O is around 0.88 eV and its energy threshold is relatively high, about 1.76 eV (see Table II). Consequently, when reaction channel (2) opens in K$^+$ + i-C$_3$H$_7$OH collisions the total energy content of the supermolecule is higher than the KH$_2$O$^+$ dissociation energy in the asymptotic reaction products channel.

For KHBr$^+$ formation, the thermal rate constants can be determined using the measured cross-section energy dependence. Since the target gas was always in thermal equilibrium conditions and assuming a Maxwell-Boltzmann[36] distribution as well as a thermal collision energy (CM) one,[39] $k(T)$ for reaction (2) has been calculated to be around 2×10^{-27} cm^{-3} molecules^{-1} s^{-1} at 303 K. This value is consistent both with the high threshold energy found in this work and with the very low lower limit of a rate constant for reaction (2) estimated by Allison and Ridge.

As stated before, the lack of reliable data about products of reaction (1) for both systems studied can be explained since the calculated dissociation energy (including ZPEs') for KC$_3$H$_6$$^+$ is 0.47 eV, while energy thresholds for these reactions are 0.71 eV and 1.76 eV, for Br and OH systems, respectively. These energies are high enough to allow the dissociation of the KC$_3$H$_6$$^+$ formed, after the adequate redistribution of the total energy content among the different vibrational modes. This idea is supported by previous studies done in our research group applying the direct quasiclassical trajectories method to similar ion-molecule collisions.[37] These calculations show that the supermolecule, after overcoming the reaction potential energy barriers (even if they have lower energies than those considered in the present study,[38]) can evolve leading to the formation of the unsaturated C$_3$H$_6$ molecule and the alkali ion as separated products, consequently causing an experimental loss of signal of KC$_3$H$_6$$^+$ although the corresponding elimination reaction did really take place.

When the collision energy increases, reaction channel (3) becomes open and the ion-molecule collision complex can dissociate into C$_3$H$_7$$^+$ and KBr or KOH in potassium-ion collisions with i-C$_3$H$_7$Br or i-C$_3$H$_7$OH targets, respectively. Decomposition of these complexes requires an effective coupling of the translational collision energy to the internal vibrational one ($T \rightarrow V$) so that enough energy can be transferred to the vibrational mode associated with the C–Br or C–OH bond stretching. According to the *ab initio* calculations, the heterolytic bond breakage takes place adiabatically on the ground singlet PES of the reacting supermolecule, ending in the formation of molecular (C$_3$H$_7$$^+$) and of the associated neutrals KBr or KOH. Excitation functions for reaction (3) in halogenated and alcohol compounds are given in Figures 1(c) and 2(b), respectively. Both show a behavior typical of reactions with an energy threshold and, while their shape

near the threshold do not allow the extrapolation of these energies with total reliability, discarding the low signals with large uncertainties the energy thresholds can be estimated to be around 2.0 eV for isopropyl bromide and 2.5 eV for isopropyl alcohol. These experimental values are lower than the *ab initio* ones (Table I) and than those calculated from formation enthalpies, particularly for the potassium-isopropyl alcohol reaction. This discrepancy could be attributed in part to restrictions imposed by the basis set functions selected, which was the same for Br and OH systems. However, for the K^+ + alcohol reaction, some tentative calculations including larger basis sets did not significantly reduce the discrepancy between experimental and calculated results. Another possible explanation could be the existence of simultaneous long-range ion-dipole and ion-induced dipole interactions, that would require the use of highest level *ab initio* calculations (such as multi-configuration or interaction configuration methods) and larger basis sets, which clearly exceed our present calculations capabilities.

Comparing cross-section values for reaction (3) with those of the adduct formation (Figures 1(a) and 2(a)) it can be seen that in the reaction of i-C_3H_7Br their values are around two order of magnitude larger than the latter ones, clearly indicating the dominance of the decomposition channel (3) over any other reactions in the halide compound. Conversely, in the case of i-C_3H_7OH, reaction (3) cross sections are about two orders of magnitude lower than those for the adduct formation. As in the case of the K^+ + i-C_3H_7Cl system,[6] reaction (3) is the most important channel, although changing chlorine by bromine reduces the measured cross-section values by around one order of magnitude. This can be due to the Br larger atomic size, which decreases the K^+ reactivity with the molecule via reaction (3) while still maintaining this reaction as the dominant one. In the case of i-C_3H_7OH, the fact that reaction (3) has a lower reactivity than adduct formation can be attributed to the stronger ion-molecule interaction which stabilizes the collision complex, and to its more complex chemical structure which hampers the adequate internal energy distribution leading to KOH separation. A clearer interpretation of these effects would require a detailed reaction dynamics calculation of the reaction systems but taking into account the large number of internal degrees of freedom involved (30 and 33 vibration modes for i-C_3H_7Br and i-C_3H_7OH, respectively) these studies are really out of our actual possibilities.

V. CONCLUSIONS

The reactivity of gas-phase collisions of ground state potassium ions with i-C_3H_7Br and i-C_3H_7OH molecules has been measured using the experimental RF-GIB technique under single collision conditions. The mass analysis of the different molecular ions produced in the ion-molecule collisions revealed the existence of different reaction channels, and the corresponding excitation functions were determined for nearly all of them in absolute units in the 0.05–10.0 eV energy range. These include the formation of the ion-molecule $[K$-i-$C_3H_7R]^+$ adducts (with R = Br, OH) and that of the $KHBr^+$ in K^+ + i-C_3H_7Br collisions. Moreover, cross-section energy dependences for the decomposition of the

$[K$-i-$C_3H_7R]^+$ adducts leading to reaction (3) have also been measured for both collisional systems. The experimental study of the above mentioned reactions has been complemented by the characterization, at the MP2 *ab initio* level, of the main topological trends of the PESs on which the reactive processes take place adiabatically. These studies reveal the formation of ion-molecule adducts essentially by non-covalent interactions. The PESs show that no potential energy barriers are involved in the formation of these non-covalent adducts, but important ones do appear along the reaction pathways leading to products, imposing relatively large energy requirements for dehydrohalogenation or dehydration reactions to proceed. From these requirements as well as from the energy calculations done for $KC_3H_6^+$ and KH_2O^+ reaction products it has been possible to justify, at least qualitatively, the impossibility to determine experimentally the corresponding excitation functions: Simply the collision energy required is higher than the asymptotic dissociation energy of both $KC_3H_6^+$ and KH_2O^+ species into K^+ and C_3H_6 or H_2O, respectively. Contrariwise, the PES topological characteristics and the $KHBr^+$ dissociation energy value justify that this products' excitation function could be measured because it can be produced below their dissociation limit. Moreover, the order of magnitude of the calculated thermal rate constant value for the corresponding reaction is in agreement with predictions made in previous studies. Calculated PESs for studied reactions also interpret, at least qualitatively, the presence of a threshold energy for the decomposition of the $[K$-i-$C_3H_7R]^+$ adducts (reaction (3)). Unfortunately the absence of analytical potential surfaces suitable for these reactions and the prohibitive computer times needed for a direct trajectory study of their dynamic calculations do not allow a full dynamics interpretation of the experimental results.

ACKNOWLEDGMENTS

[1]K. L. Williams, I. T. Martin, and E. R. Fisher, J. Am. Soc. Mass Spectrom. **13**, 518 (2002).

[2]M. H. Rees, in *Physics and Chemistry of the Upper Atmosphere* (Cambridge University Press, Cambridge, 1989), pp. 278–281.

[3]T. B. McMahon and G. Ohanessian, Chem. – Eur. J. **6**, 2931 (2000).

[4]W. Klemperer and V. Vaida, Proc. Natl. Acad. Sci. U.S.A. **103**, 10584 (2006).

[5]J. de Andrés, J. M. Lucas, M. Albertí, J. M. Bofill, A. Belyaev, and A. Aguilar, J. Chem. Phys. **137**, 154202 (2012).

[6]J. Aguilar, J. M. Lucas, J. de Andrés, M. Albertí, D. Bassi, and A. Aguilar, J. Chem. Phys. **138**, 184310 (2013).

[7]M. Sabidó, J. de Andrés, J. Sogas, M. Albertí, J. M. Bofill, I. Rabadán, and A. Aguilar, Eur. Phys. J. D **47**, 63 (2008).

[8]M. Sabidó, J. de Andrés, J. Sogas, J. M. Lucas, M. Albertí, J. M. Bofill, and A. Aguilar, Phys. Chem. Chem. Phys. **7**, 310 (2005).

[9]J. Allison and D. P. Ridge, J. Am. Chem. Soc. **98**, 7445 (1976).

[10]J. Allison and D. P. Ridge, J. Am. Chem. Soc. **101**, 4998 (1979).

[11]R. D. Wieting, R. H. Staley, and J. L. Beauchamp, J. Am. Chem. Soc. **97**, 924 (1975).

[12]W. R. Creasy and J. M. Farrar, J. Phys. Chem. **89**, 3952 (1985).

[13]W. R. Creasy and J. M. Farrar, J. Chem. Phys. **87**, 5280 (1987).

[14]M. Sabido, J. M. Lucas, J. de Andrés, J. Sogas, M. Albertí, A. Aguilar, D. Bassi, D. Ascenzi, P. Franceschi, P. Tosi, and F. Pirani, Chem. Phys. Lett. **442**, 28 (2007).

[15]J. M. Lucas, J. de Andrés, J. Sogas, M. Albertí, J. M. Bofill, D. Bassi, D. Ascenzi, P. Tosi, and A. Aguilar, J. Chem. Phys. **131**, 024306 (2009).

[16]J. M. Lucas, J. de Andrés, M. Albertí, J. M. Bofill, D. Bassi, and A. Aguilar, Phys. Chem. Chem. Phys. **12**, 13646 (2010).

[17]J. Aguilar, J. M. Lucas, J. de Andrés, M. Albertí, D. Bassi, and A. Aguilar, Phys. Chem. Chem. Phys. **13**, 18581 (2011).

[18]J. H. Batey and J. M. Tedder, J. Chem. Soc., Perkin Trans. 2 **1983**, 1263.

[19]K. M. Ervin and P. B. Armentrout, J. Chem. Phys. **83**, 166 (1985).

[20]P. J. Chantry, J. Chem. Phys. **55**, 2746 (1971).

[21]C. Lifshitz, R. L. C. Wu, T. O. Tiernan, and D. T. Terwilliger, J. Chem. Phys. **68**, 247 (1978).

[22]C. G. Schlier, Chem. Phys. **126**, 73 (1988).

[23]E. López, J. M. Lucas, J. de Andrés, M. Albertí, J. M. Bofill, D. Bassi, and A. Aguilar, Phys. Chem. Chem. Phys. **13**, 15977 (2011).

[24]H. Koizumi and P. B. Armentrout, J. Chem. Phys. **119**, 12819 (2003).

[25]C. M. Aikens, S. P. Webb, R. L. Bell, G. D. Fletcher, M. W. Schmidt, and M. S. Gordon, Theor. Chem. Acc. **110**, 233 (2003).

[26]M. J. Frisch, G. W. Trucks, H. B. Schlegel *et al.*, GAUSSIAN03, Revision E.01, Gaussian Inc.,Wallingford, CT, 2004.

[27]M. S. Gordon, M. W. Schmidt, C. E. Dykstra, G. Frenking, K. S. Kim, and G. E. Scuseria, *Theory and Applications of Computational Chemistry: The first Forty Years* (Elsevier, 2005), p. 1167.

[28]K. Fukui, J. Phys. Chem. **74**, 4161 (1970).

[29]C. Gonzalez and H. B. Schlegel, J. Chem. Phys. **90**, 2154 (1989).

[30]P. J. Stephens, K. J. Jalkanen, and R. W. Kawiecki, J. Am. Chem. Soc. **112**, 6518 (1990).

[31]M. M. C. Ferreira, J. Mol. Struct. **294**, 75 (1993).

[32]J. M. Lucas, J. de Andrés, M. Albertí, J. M. Bofill, D. Bassi, and A. Aguilar, Phys. Chem. Chem. Phys. **12**, 13646 (2010).

[33]J. M. Lucas, J. de Andrés, E. López, M. Albertí, J. M. Bofill, D. Bassi, D. Ascenzi, P. Tosi, and A. Aguilar, J. Phys. Chem. A **113**, 14766 (2009).

[34]See http://webbock.nist.gov/chemisty/ for thermodynamic magnitudes.

[35]*CRC Handbook of Chemistry and Physics*, 77th ed., edited by D. R. Lide (CRC, Boca Raton, FL, 1996).

[36]R. D. Levine, *Molecular Reaction Dynamics* (Cambridge University Press, 2005), pp. 81, 92, 93.

[37]J. Aguilar, J. de Andrés, J. M. Lucas, M. Albertí, F. Huarte-Larrañaga, D. Bassi, and A. Aguilar, AIP Conf. Proc. **1501**, 1340 (2012).

[38]Javier Aguilar, Ph.D. thesis dissertation, University of Barcelona, 2014.

[39]J. I. Steinfeld, J. S. Francisco, and W. Hase, *Chemical Kinetics and Dynamics* (Prentice-Hall, Inc., New Jersey, 1989), pp. 205, 272.